BBA - Molecular Basis of Disease 1865 (2019) 1782–1792

Contents lists available at ScienceDirect

BBA - Molecular Basis of Disease

journal homepage: www.elsevier.com/locate/bbadis

Aldehyde dehydrogenase 2 deficiency promotes atherosclerotic plaque instability through accelerating mitochondrial ROS-mediated vascular smooth muscle cell senescence

Hong Zhu[a,1], Zeng Wang[a,1], Zhen Dong[b,1], Cong Wang[b], Quan Cao[b], Fan Fan[b], Jingjing Zhao[c], Xiangwei Liu[b], Meng Yuan[b], Xiaolei Sun[a], Xiuhua Peng[d], Yunzeng Zou[a], Jingmin Zhou[b], Junbo Ge[a], Xiaohui Zhou[d,*], Yingmei Zhang[b,*]

[a] Shanghai Institute of Cardiovascular Disease, Zhongshan Hospital & Institute of Biomedical Sciences, Fudan University, Shanghai 200032, China
[b] Shanghai Institute of Cardiovascular Diseases, Department of Cardiology, Zhongshan Hospital, Fudan University Shanghai 200032, China
[c] Department of Cardiology, First Affiliated Hospital, Sun Yat-sen University, Guangzhou 510080, China
[d] Shanghai Public Health Clinical Center, Fudan University, Shanghai 200032, China

ARTICLE INFO

Keywords:
ALDH2
Atherosclerosis
Macrophage
VSMC
Senescence
Mitochondrial ROS

ABSTRACT

Previous evidence has indicated a beneficial role for aldehyde dehydrogenase 2 (ALDH2) in suppressing atherosclerotic plaque progression and instability. However, the underlying mechanism remains somewhat elusive. This study was designed to examine the effect of ALDH2 deficiency on high-cholesterol diet-induced atherosclerotic plaque progression and plaque vulnerability in atherosclerosis-prone ApoE knockout ($ApoE^{-/-}$) mice with a focus on foam cell formation in macrophages and senescence of vascular smooth muscle cells (VSMCs). Serum lipid profile, plaque progression, and plaque vulnerability were examined in $ApoE^{-/-}$ and ALDH2/ApoE double knockout ($ALDH2^{-/-}ApoE^{-/-}$) mice after high-cholesterol diet intake for 8 weeks. ALDH2 deficiency increased the serum levels of triglycerides while it decreased levels of total cholesterol and high-density lipoprotein cholesterol. Unexpectedly, ALDH2 deficiency reduced the plaque area by 58.9% and 37.5% in aorta and aortic sinus, respectively. Plaque instability was aggravated by ALDH2 deficiency along with the increased necrotic core size, decreased collagen content, thinner fibrous cap area, decreased VSMC content, and increased macrophage content. In atherosclerotic lesions, ALDH2 protein was located in both macrophages and VSMCs. Further results revealed downregulated ALDH2 expression in aorta of aged $ApoE^{-/-}$ mice compared with young mice. However, in vitro study suggested that ALDH2 expression was upregulated in bone marrow-derived macrophages (BMDMs) with an opposite effect in VSMCs following 80 μg/ml oxidized low-density lipoprotein (oxLDL) treatment. Interestingly, ALDH2 deficiency displayed little effect in oxLDL-induced foam cell formation from BMDMs, while ALDH2 knockdown by siRNA and ALDH2 overexpression by lentivirus infection promoted and retarded oxLDL-induced VSMC senescence, respectively. Mechanistically, ALDH2 mitigated oxLDL-induced overproduction of mitochondrial reactive oxygen species (mROS) and activation of downstream p53/p21/p16 pathway. Clearance of mROS by mitoTEMPO significantly reversed the promotive effect of ALDH2 knockdown on VSMC senescence. Taken together, our data revealed that ALDH2 deficiency suppressed atherosclerotic plaque area while facilitating plaque instability possibly through accelerating mROS-mediated VSMC senescence.

This article is part of a Special Issue entitled: Genetic and epigenetic regulation of aging and longevity edited by Jun Ren & Megan Yingmei Zhang.

* Corresponding authors at: Shanghai Institute of Cardiovascular Disease, Department of Cardiology, Zhongshan Hospital, Fudan University, Shanghai 200032, China.
E-mail addresses: zhouxiaohui@shphc.org.cn (X. Zhou), zhang.yingmei@zs-hospital.sh.cn (Y. Zhang).
[1] Contributed equally to this work.

https://doi.org/10.1016/j.bbadis.2018.09.033
Received 31 July 2018; Received in revised form 26 September 2018; Accepted 27 September 2018
Available online 11 October 2018
0925-4439/

1. Introduction

Atherosclerosis is one of the primary causes of cardiovascular diseases, including coronary artery disease, myocardial infarction, and stroke. Formation and progression of atherosclerotic lesions is a chronic pro-inflammatory response of arterial wall, characterized by endothelial dysfunction, infiltration of inflammatory cells, formation of lipid-enriched necrotic core and rupture-prone fibrotic cap [1]. Vulnerable atherosclerotic plaque is recognized as the main culprit of thrombosis of coronary artery and unpredictable event of acute coronary syndrome (ACS), manifested as enlarged necrotic core size, thin fibrous caps, reduced collagen content, and increased filtration of inflammatory cells [2,3]. As the major components in atherosclerotic lesions, macrophages and vascular smooth muscle cells (VSMCs) play critical roles in the pathogenesis of atherosclerosis. Uncontrolled accumulation of lipoproteins such as oxidized-low density lipoproteins (oxLDLs) promotes transition of macrophages into lipid-rich foam cells, resulting in the lesion expansion and plaque instability [4]. The macrophage-derived chemoattractants promote the migration of VSMC from the arterial wall into the lesion, where they secrete extracellular matrix proteins and form fibrous cap with a prominent role in the maintenance of plaque stability [5]. It is well-known that apoptosis of VSMC predisposes vulnerability in atherosclerotic plaque [6]. Apart from apoptosis, recent studies have revealed that VSMC senescence also promotes atherosclerotic plaque vulnerability [7,8]. VSMC senescence is an important part of vascular aging, which could be simply defined as a consequence of natural physical stress and age-dependent change of the vascular structure and function, resulting in decreased arterial compliance and increased arterial stiffening [9].

A growing number of evidence suggests that several cholesterol oxidation products, such as oxysterols and 4-hydroxy-2-nonenal (4-HNE), the major proatherogenic components of oxLDLs, significantly contribute to atherosclerotic plaque progression and vulnerability [10].

Mitochondrial aldehyde dehydrogenase (ALDH2), mostly known for its role in ethanol metabolism, is a key enzyme involved in the degradation of toxic reactive acetaldehydes, such as 4-HNE and malondialdehyde (MDA), into non-toxic acetic acid [11]. Findings from our laboratory and others revealed a beneficial role of ALDH2 in protecting against cardiovascular diseases (CVDs), such as coronary heart disease [12,13], ischemia heart disease [14,15], alcoholic cardiomyopathy [16], diabetic cardiomyopathy [17], and stroke [18,19]. The beneficial effect of ALDH2 in CVDs might be mediated through regulation of oxidative stress, cell metabolism, inflammatory response, apoptosis and autophagy [20,21]. Recently, the beneficial role of ALDH2 in experimental atherosclerosis was revealed [22,23]. Stachowicz and colleagues reported that mitochondrial ALDH2 activation using a specific ALDH2 activator Alda-1 decreased atherogenic plaque area without any influence on lipid profile or plaque vulnerability in atherosclerosis-prone ApoE knockout ($ApoE^{-/-}$) mice fed chow diet [22]. On the other hand, Pan and coworkers revealed that ALDH2 knockdown using lentivirus infection resulted in increased atherogenic plaque area and instability in $ApoE^{-/-}$ mice fed high-cholesterol diet, along with the aggravated inflammation in endothelial cells, while ALDH2 overexpression using lentivirus displayed opposite effects [23]. Nonetheless, none of these two studies depicted the precise association between genetic ALDH2 deficiency and atherosclerotic lesion progression, in particular the underlying mechanisms involving macrophage and VSMC function.

Given that nearly 40% of loss-of-function mutation of ALDH2 presents in east Asians [24], it is pertinent to elucidate whether ALDH2 deficiency aggravates atherosclerotic plaque progression and vulnerability. To this end, we generated a double knockout $ALDH2^{-/-}ApoE^{-/-}$ murine model to elucidate the precise effect of ALDH2 deficiency on the progression of atherosclerosis and plaque vulnerability, with a special focus on macrophage foam cell formation and VSMC senescence.

2. Methods and materials

2.1. $ALDH2^{-/-}ApoE^{-/-}$ mouse generation and high-cholesterol diet intake

$ApoE^{-/-}$ mice (with a C57BL/6 background) were obtained from Beijing Vital River Laboratory Animal Technology Company. The $ALDH2^{-/-}ApoE^{-/-}$ double knockout mice were generated by breeding $ALDH2^{-/-}$ mice (also on C57BL/6 background) with $ApoE^{-/-}$ mice as previously reported [25]. The resulting heterozygous F1 generation were interbred with each other to produce homozygote $ALDH2^{-/-}ApoE^{-/-}$ mice. The genotypes of mice were identified using agarose gel electrophoresis and Western blotting. Mice were maintained on a 12/12-hour dark/light cycle in an air-conditioned room (22.5 ± 0.5 °C, 50 ± % humidity) with access to diet and water ad libitum in the Animal House of Zhongshan Hospital, Fudan University (Shanghai, China). Two-month-old $ALDH2^{+/+}ApoE^{-/-}$ mice and $ALDH2^{-/-}ApoE^{-/-}$ mice were fed high-cholesterol diet (1.25% cholesterol and 0.5% cholic acid) for 8 weeks. All animals were handled following the Regulations of Experimental Animal Administration issued by the State Committee of Science and Technology of the People's Republic of China.

2.2. Animal sacrifice and serum lipoprotein analysis

After an eight-week high-cholesterol diet feeding, mice were sedated using pentobarbital sodium (80 mg/kg) and blood was collected from inferior vena cava. Animals were sacrificed using the exsanguination procedure. Blood was centrifuged at 3000 rpm for 10 min at 4 °C. Serum total cholesterol (TC), triglycerides (TG) and high density lipoprotein-cholesterol (HDL-C) levels were measured using commercial kits (Biosino Bio-Technology and Science Inc.).

2.3. Evaluation of atherosclerotic lesion development

Following collection of blood, the circulatory system was washed with PBS and then fixed with PBS containing 4% paraformaldehyde. Aorta was then excised from the root to abdominal area. Connective tissues were removed underneath the dissecting microscope. Aorta were cut longitudinally and “en face” plaque area was visualized using oil red O (ORO, Sigma) staining, before being photographed with a digital camera and quantified by Image J software. The heart and ascending aorta were embedded in optimal cutting temperature (OCT) compound (Sakura) and snap-frozen on liquid nitrogen. For the analysis of lesion formation in aortic sinus, serial (7-μm thickness) cross-sections were collected from the origin of aortic valve leaflets. Every tenth sections were stained with ORO to detect lipid deposition. Atherosclerotic lesion areas were quantified using Image J software and were reported as the average ORO staining area per section in the first ten sections for each mouse.

2.4. Histological examination

Frozen sections of atherosclerotic lesion at the aortic sinus were employed for the histological examination. H&E staining, Masson staining and Sirus red staining were used to detect necrotic core size, collagen content, and fibrous cap area, respectively.

2.5. Immunofluorescence and immunohistochemistry

For immunofluorescence staining, formaldehyde-fixed sections were incubated with primary antibodies at 4 °C overnight. Macrophages and VSMCs in atherosclerotic lesions were detected with the rat anti-mouse CD68 (Abcam) and rat anti-mouse α-SMA antibody (Sigma), respectively, and were co-stained with the rabbit anti-mouse ALDH2 antibody (Abgent). Samples were then incubated with Alexa Fluor 488 or 594

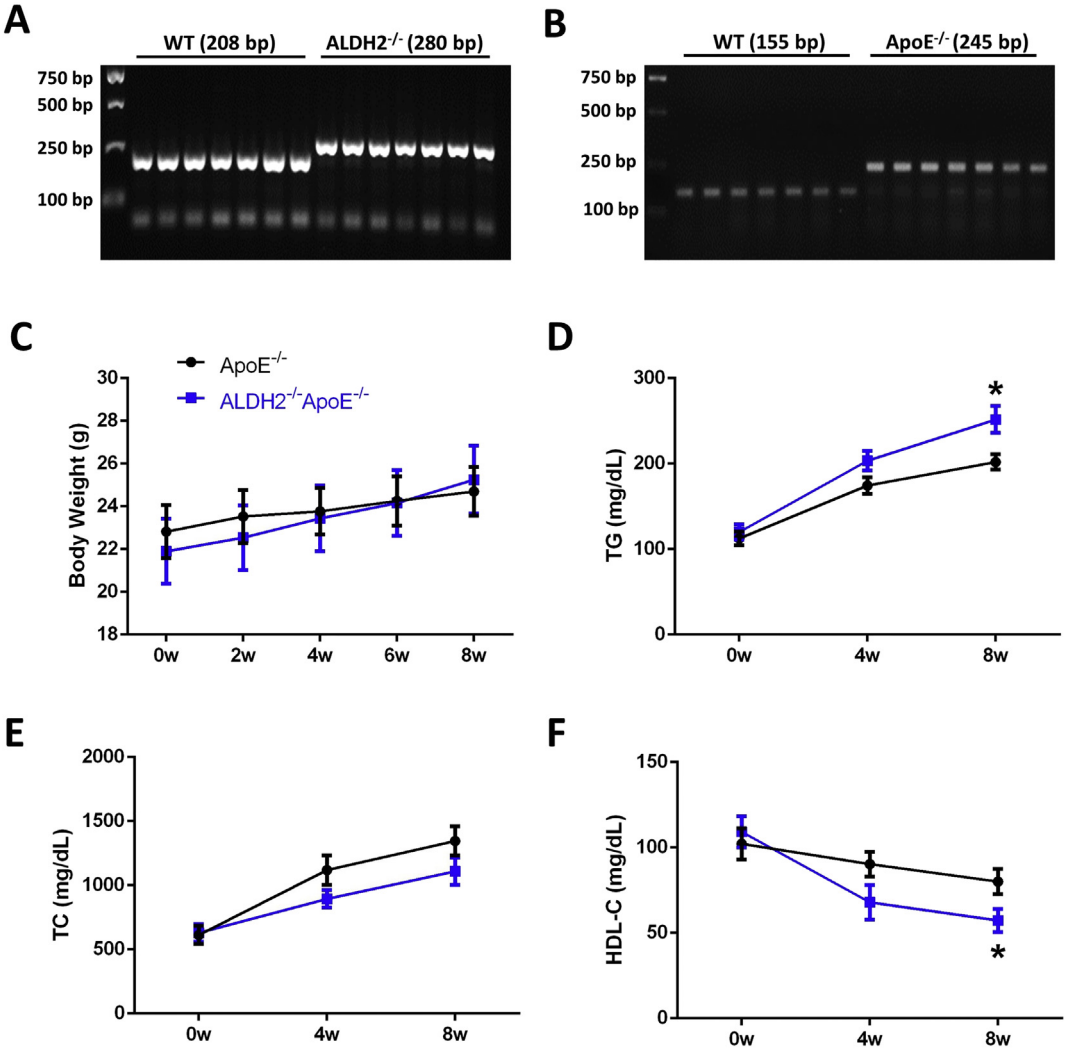

Fig. 1. Body weight, serum TG, TC and HDL-C concentrations in ApoE$^{-/-}$ and ALDH2$^{-/-}$ApoE$^{-/-}$ mice. A, B: Representative agarose gel electrophoresis pictures of ALDH2$^{-/-}$ApoE$^{-/-}$ mice; C: Body weight at baseline, 2 weeks, 4 weeks, 6 weeks, and 8 weeks after high-cholesterol diet challenge; D: Serum TG concentration at baseline, 4 weeks, and 8 weeks after high-cholesterol diet challenge; E: Serum TC concentration at baseline, 4 weeks, and 8 weeks after high-cholesterol diet challenge; F: Serum HDL-C concentration at baseline, 4 weeks, and 8 weeks after high-cholesterol diet challenge. Mean ± SEM, $n = 12$ for both ApoE$^{-/-}$ and ALDH2$^{-/-}$ApoE$^{-/-}$ groups. *$p < 0.05$ vs. ApoE$^{-/-}$ group.

labeled secondary antibodies (Invitrogen). Nuclei were stained with 4′, 6-diamidino-2-phenylindole (DAPI, Sigma). Confocal images were obtained by using a Zeiss LSM 510 microscope. For immunohistochemistry staining, endogenous peroxidase activity was quenched with 3% hydrogen peroxide. Then sections were incubated with primary antibodies at 4 °C overnight. Macrophages and VSMCs were detected by using rabbit anti-mouse F4/80 antibody (Abcam) and rabbit anti-mouse α-SMA antibody (Abcam), respectively. A streptavidin-biotin complex (SABC) kit (Wuhan Boster Biological Technology, Wuhan, China) and DAB substrate (Wuhan Boster Biological Technology, Wuhan, China) were then used to develop the brown reaction product. Slides were counterstained with hematoxylin. Pictures were obtained using a Leica microscope. Images were analyzed using the Image-Pro Plus software.

2.6. Western blot analysis

Aorta and cells were homogenized and sonicated in a lysis buffer containing 20 mM Tris (pH 7.4), 150 mM NaCl, 1 mM EDTA, 1 mM EGTA, 1% Triton, 0.1% sodium dodecyl sulfate (SDS), and a protease inhibitor cocktail. Samples were incubated with the primary anti-ALDH2 (Abcam), anti-p53 (Abcam), anti-p21 (Abcam), anti-p16 (CST), anti-β-actin (CST), and anti-GAPDH (CST) antibodies. Membranes were then incubated with horseradish peroxidase (HRP)-coupled secondary antibodies (Aksomics). After immunoblotting, films were scanned and detected using a Bio-Rad Calibrated Densitometer. Intensity of immunoblot bands was normalized to the loading control (β-actin or GAPDH).

2.7. Cell culture and lentivirus infection

Bone marrow derived macrophages (BMDMs) were obtained as described [26]. In briefly, mice were euthanized using overdose anesthetic and bone marrow cells were obtained from hind limbs. Cells were plated in RPMI-1640 containing 20% FBS and stimulated by M-CSF for 7 days before usage. Human umbilical vein smooth muscle cells were purchased from ScienCell (Cat No: 8020, ScienCell) and were cultured in Smooth Muscle Cell Medium (Cat No: 1101, ScienCell) supplemented with 100 U/ml penicillin, 100 μg/ml streptomycin, smooth muscle cell growth supplement (Cat. No. 1152, ScienCell), and 5% FBS. Lentivirus vectors were generated as described [14] and were employed to generate the ALDH2 overexpression in VSMCs. Normal control siRNA and ALDH2 siRNA were generated as previously reported [14]. Transfection was performed using riboFECT™ CP transfection kit in serum-free

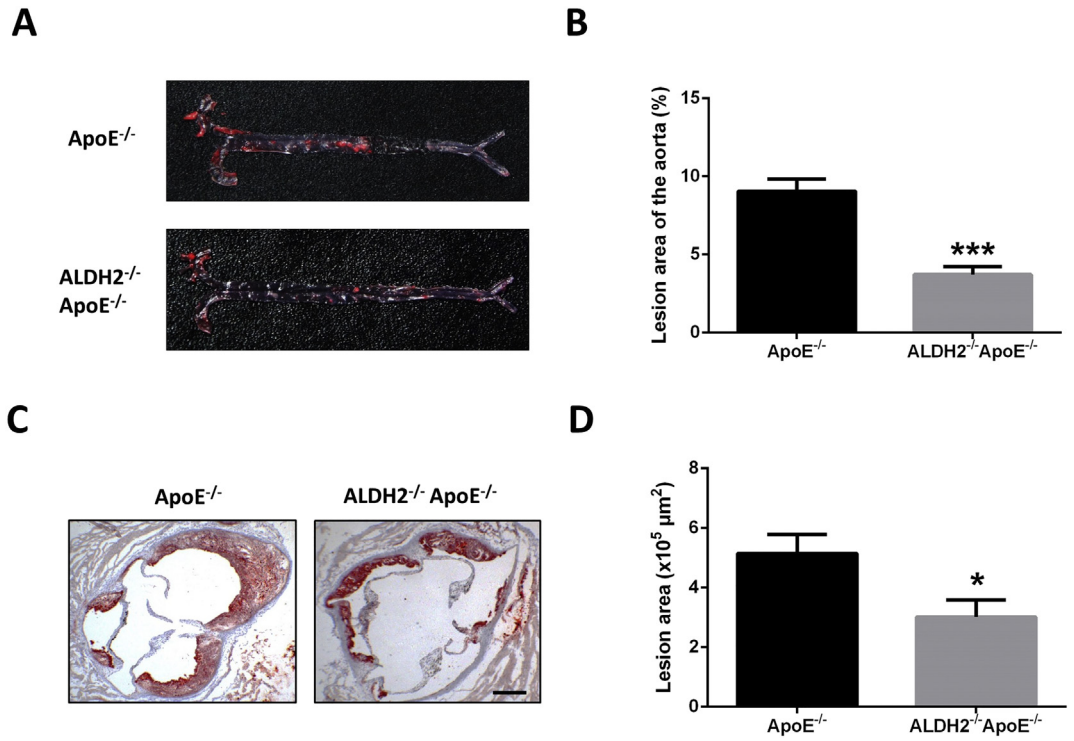

Fig. 2. Lesion area at the aorta and aortic sinus in ApoE$^{-/-}$ and ALDH2$^{-/-}$ApoE$^{-/-}$ mice. A: Representative pictures of oil red O stained lesions at the aorta; B: Statistical results of the lesion area of aorta; C: Representative pictures of oil red O stained lesions at the aortic sinus; D: Statistical results of the lesion area of aorta, scale bar = 200 μm. Mean ± SEM, $n = 12$ for both ApoE$^{-/-}$ and ALDH2$^{-/-}$ApoE$^{-/-}$ groups. *$p < 0.05$, ***$p < 0.001$ vs. ApoE$^{-/-}$ group.

medium (RiboBio) following manufacturer's protocol.

2.8. Analysis of foam cell formation

BMDMs were plated in RPMI-1640 containing 1% FBS and 80 μg/ml oxLDL for 24 h. Cells were fixed for 30 min in 4% paraformaldehyde, rinsed in ddH2O, washed in 60% isopropanol for 5 min, stained with 0.3% ORO solution for 15 min, and then counterstained with hematoxylin for 1 min. Stained cells were eluted with isopropanol, and the resultant supernatant was collected. Optimal density was measured at 540 nm. BMDMs were also incubated with 40 μg/ml DiI-oxLDL for 6 h and were fixed in phosphate-buffered 4% paraformaldehyde for 10 min. Fluorescent signals were detected using the immunofluorescence microscopy.

2.9. SA-β-gal staining

SA-b-gal activity was determined using a commercial kit (CST) according to the manufacturer's instructions. Briefly, cells were fixed in 2% formaldehyde containing 0.2% glutaraldehyde for 15 min and were washed with PBS twice. Samples were incubated at 37 °C for 24 h in a staining solution containing X-gal in dimethylformamide (1 mg/ml), potassium ferrocyanide (5 nM), potassium ferricyanide (5 nM), citric acid/sodium phosphate (40 mM), NaCl (0.15 M), and $MgCl_2$ (2 mM) with a pH of 5.9. Cells were photographed using a light microscope. Cells with blue color were considered being SA-β-gal positive.

2.10. DHE staining

Following challenge with 80 μg/ml oxLDL for 72 h, DHE (10 μM) were added and incubated for 30 min. Cells were washed with cold 1 × PBS and fluorescent signals were captured using a fluorescent microscope (Olympus).

2.11. Data analyses

Data were presented as means ± SEM. Data were analyzed using the unpaired Student *t*-test or one-way ANOVA followed by a Tukey post hoc analysis. All statistical analyses were performed using Graphpad Prism 6.0, and a p value < 0.05 was considered statistically significant.

3. Results

3.1. Body weight and serum lipid profile in ApoE$^{-/-}$ and ALDH2$^{-/-}$ApoE$^{-/-}$ mice

The ALDH2$^{-/-}$ApoE$^{-/-}$ mice were generated and identified with agarose gel electrophoresis (Fig. 1A and B). Both ApoE$^{-/-}$ and ALDH2$^{-/-}$ApoE$^{-/-}$ mice were challenged with high-cholesterol diet for 8 weeks. Body weight was monitored at baseline, 2 weeks, 4 weeks, 6 weeks, and 8 weeks after high-cholesterol diet intake. Our results exhibited little differences in body weight between two groups (Fig. 1C). Serum lipid profile including TG, TC and HDL-C was measured using commercial kits. High-cholesterol intake increased serum TG and TC levels while decreasing HDL-C levels (Fig. 1D–F). Interestingly, elevated TG levels were more pronounced in ALDH2$^{-/-}$ApoE$^{-/-}$ mice compared with ApoE$^{-/-}$ mice (Fig. 1D). However, serum TC and HDL-C levels were lower in ALDH2$^{-/-}$ApoE$^{-/-}$ mice compared with ApoE$^{-/-}$ mice (Fig. 1E–F). These data revealed that ALDH2 deficiency in ApoE$^{-/-}$ mice might affect lipid metabolism, manifested as elevated TG levels and decreased levels of TC and HDL-C.

3.2. Effect of ALDH2 deficiency on atherosclerotic lesion formation

Several studies revealed the protective role of ALDH2 in inhibiting atherosclerotic plaque progression using the specific ALDH2 activator Alda-1 [22] and lentivirus-induced ALDH2 overexpression [23]. Nonetheless, none of these studies were conducted from a genetic

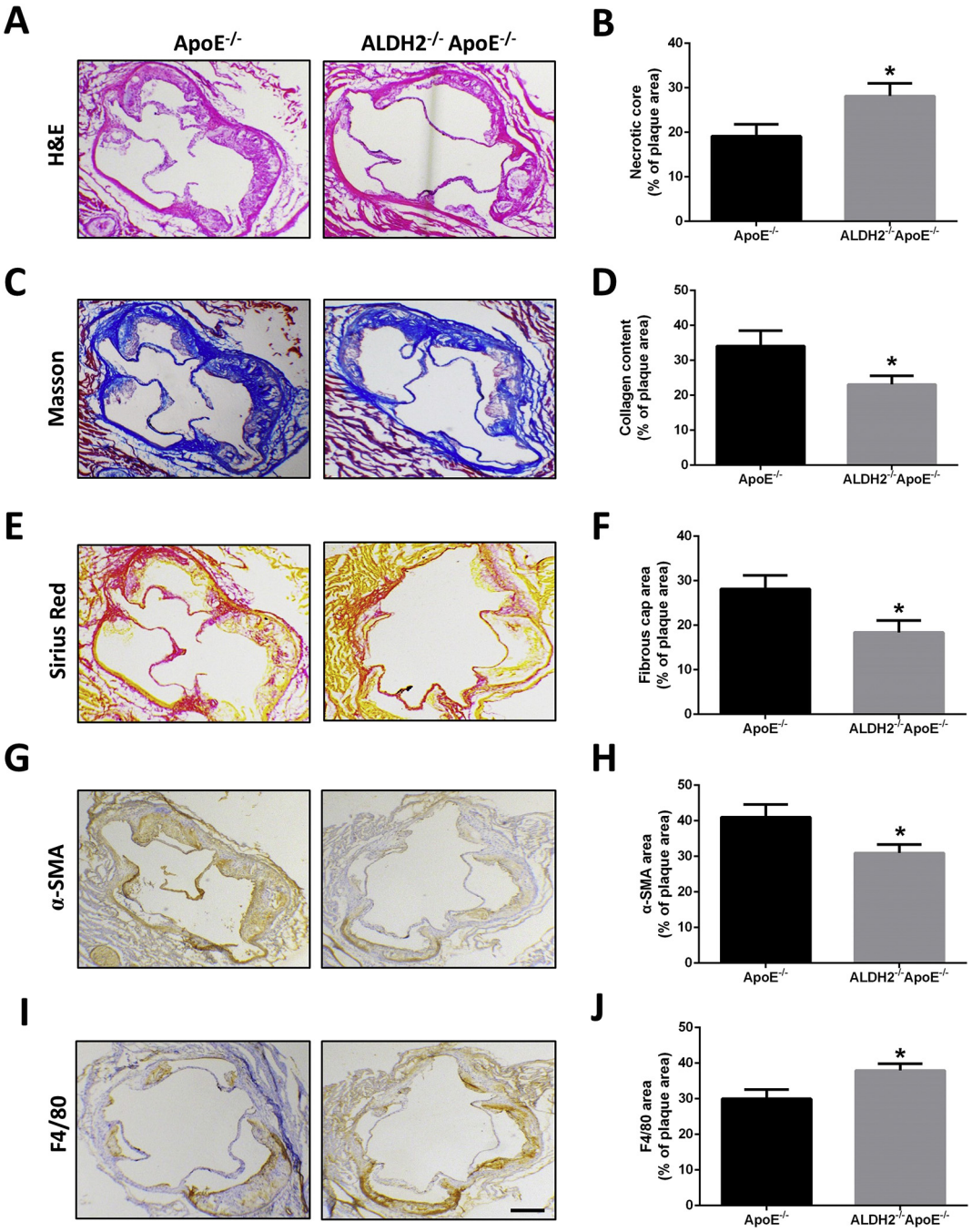

Fig. 3. Lesion stability analyses in aortic sinus in ApoE$^{-/-}$ and ALDH2$^{-/-}$ApoE$^{-/-}$ mice. A, C, E, G, I: Representative pictures of H&E staining, Masson staining, Sirius red staining, α-SMA and F4/80 immunohistochemistry staining in the lesions at the aortic sinus; B, D, F, H, J: Statistical results of necrotic core size (%), collagen content (%), fibrous cap area (%), α-SMA positive area (%), and F4/80 positive area (%) in the lesions at the aortic sinus. Scale bar = 200 μm. Mean ± SEM, $n = 6$ for both ApoE$^{-/-}$ and ALDH2$^{-/-}$ApoE$^{-/-}$ groups. *$p < 0.05$ vs. ApoE$^{-/-}$ group.

perspective. To elucidate the effect of genetic ALDH2 deficiency on atherosclerotic lesion formation, ORO staining was used to visualize the lesion area in both aorta and aortic sinus in ApoE$^{-/-}$ and ALDH2$^{-/-}$ApoE$^{-/-}$ mice fed high-cholesterol diet for 8 weeks. Unexpectedly, ALDH2$^{-/-}$ApoE$^{-/-}$ mice showed a significantly decrease in *en face* plaque area in aorta (9.06 ± 0.77% vs 3.72 ± 0.50%, $p < 0.001$), and aortic sinus (5.15 ± 0.64 vs 3.02 ± 0.56, $\times 10^5\,\mu m^2$, $p < 0.05$) compared with those from the ApoE$^{-/-}$ mice (Fig. 2A–D).

3.3. Effect of ALDH2 deficiency on atherosclerotic plaque stability

Since plaque stability is a more important predicting indicator for ACS as opposed to plaque area, atherosclerotic plaque vulnerability was monitored at the aortic sinus by histological and immunohistochemical (IHC) staining. Interestingly, H&E staining revealed that ALDH2 deficiency showed an overly bigger necrotic core size compared with control mice despite of a smaller plaque area (Fig. 3A–B). Masson staining and Sirius red staining revealed a thinner fibrous cap and less collagen content in the atherosclerotic plaque in ALDH2$^{-/-}$ApoE$^{-/-}$ mice compared with ApoE$^{-/-}$ mice (Fig. 3C–F). Given the essential role for extracellular matrix proteins including collagen in the fibrous cap mainly secreted by VSMCs, the percentage of VSMCs was measured in the plaque area. Our results revealed a remarkable reduced a-SMA positive VSMC area in the plaque in ALDH2$^{-/-}$ApoE$^{-/-}$ mice

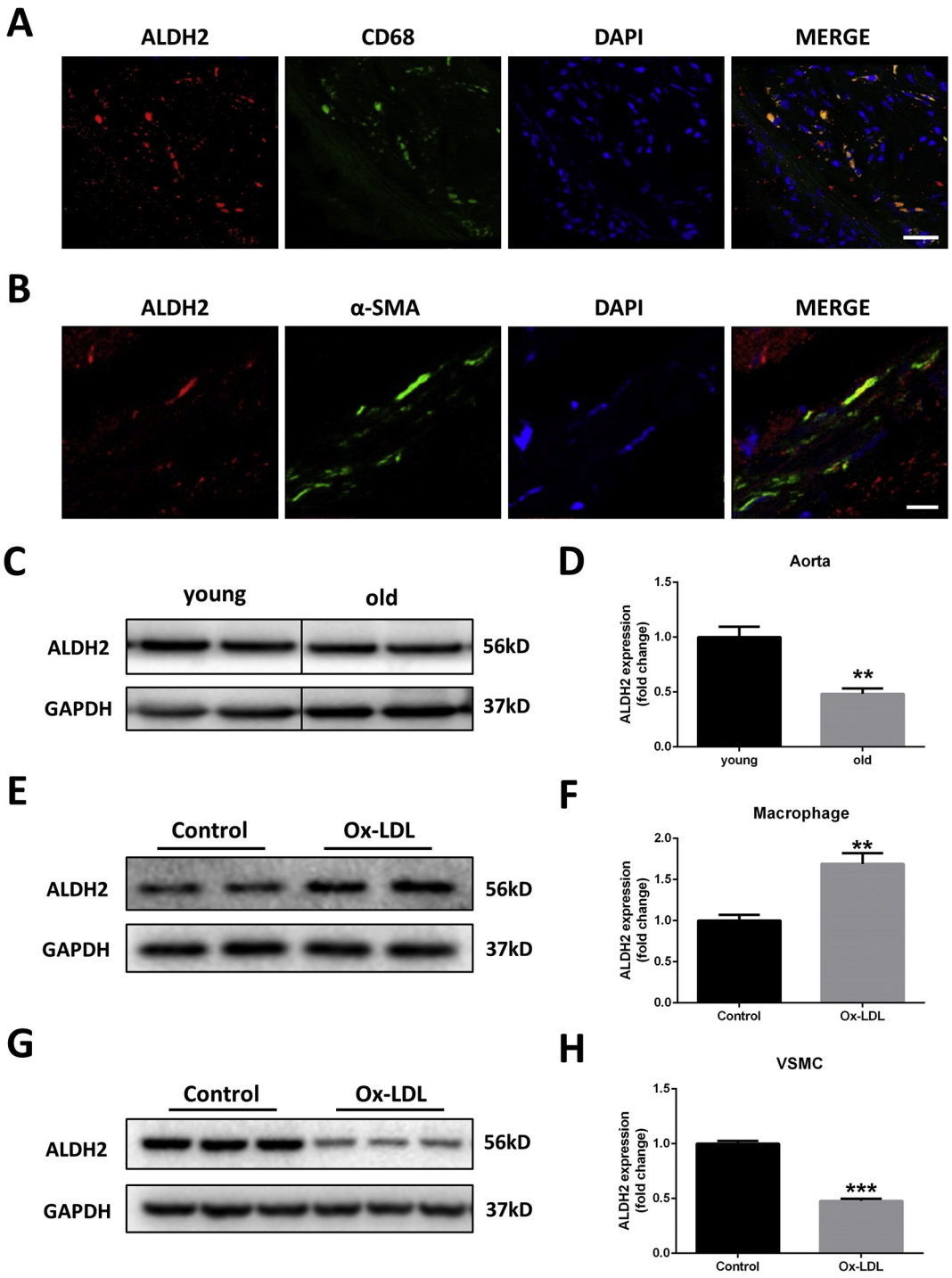

Fig. 4. ALDH2 expression in advanced atherosclerotic lesions. A: Representative pictures of co-staining of ALDH2 and CD68 in the lesions at the aortic sinus, scale bar = 50 μm; B: Representative pictures of co-staining of ALDH2 and α-SMA in the lesions at the aortic sinus, scale bar = 25 μm; C, E, G: ALDH2 expression level in aortas of young (2 month-old) and old-aged (16 month-old) ApoE$^{-/-}$ mice, and oxLDL-treated BMDMs and VSMCs; D, F, H: Statistical analyses of ALDH2 expression. Mean ± SEM, n = 4–6 for all groups. $^{**}p < 0.01$, $^{***}p < 0.001$.

compared with ApoE$^{-/-}$ mice (Fig. 3G–H). Given that plaque vulnerability is highly associated with macrophage filtration, F4/80 positive cell was detected by IHC staining and the results depicted that ALDH2 deficiency significantly increased F4/80 positive macrophages area within the plaque (Fig. 3I–J). Collectively, these data revealed that ALDH2 deficiency in ApoE$^{-/-}$ mice led to more unstable atherosclerotic plaque than that of ApoE$^{-/-}$ mice.

3.4. ALDH2 expression in advanced atherosclerotic lesions

Since both VSMC and macrophage play key roles in dictating atherosclerotic plaque stability, immunofluorescence staining was used to detect the location of ALDH2 in both macrophages and VSMCs in atherosclerotic lesions. The results clearly suggested that ALDH2 was expressed in both macrophages and VSMCs (Fig. 4A–B). We further examined ALDH2 expression in the advanced atherosclerotic lesions using Western blotting. Compared with young (2 month-old) ApoE$^{-/-}$

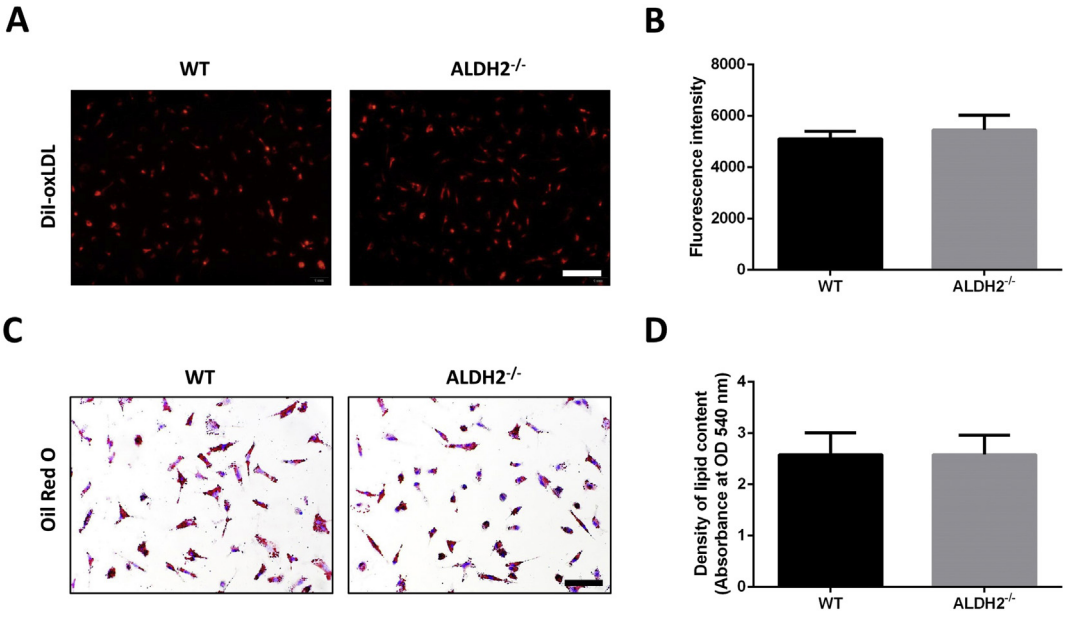

Fig. 5. Foam cell formation detection in BMDMs obtained from both WT and ALDH2$^{-/-}$ mice. A: Representative pictures of DiI-oxLDL staining after 80 μg/ml oxLDL treatment for 6 h, scale bar = 100 μm; B: Statistical analyses of the fluorescent intensity of DiI-oxLDL staining; C: Representative pictures of ORO staining after 80 μg/ml oxLDL treatment for 24 h, scale bar = 50 μm; D: Statistical analyses of the density of lipid content. Mean ± SEM, n = 6 for all groups.

mice, ALDH2 expression in aorta was significantly downregulated in aged (16 month-old) ApoE$^{-/-}$ mice (Fig. 4C–D), which was in line with the previous report study [23]. These findings favor the decrease of ALDH2 expression in atherosclerosis. To elucidate the specific cell type participating in the pathogenesis of atherosclerosis, we employed an in vitro model through stimulating both macrophages and VSMCs with oxLDL prior to assessment of ALDH2 levels. Interestingly, ALDH2 increased significantly after 80 μg/ml oxLDL treatment for 24 h in BMDMs (Fig. 4E–F), while decreased in VSMCs treated with 80 μg/ml oxLDL treatment for 72 h (Fig. 4G–H). Collectively, these results revealed downregulated ALDH2 expression in the advanced atherosclerotic lesions during the progression of atherosclerosis and in oxLDL-treated VSMCs while it was increased in oxLDL-treated macrophages. These data suggested a regulatory role of ALDH2 in the pathogenesis of atherosclerosis.

3.5. Effect of ALDH2 deficiency on oxLDL-induced foam cell formation in BMDMs

Accumulation of macrophages in atherosclerotic lesions and subsequently formation of the lipid-enriched foam cells serve as a critical step in the pathogenesis of atherosclerosis [4,27]. We tested whether ALDH2 deficiency affected foam cell formation. First, BMDMs were obtained from WT mice and ALDH2$^{-/-}$ mice. Then BMDMs were incubated with 40 μg/ml DiI-oxLDL for 6 h to examine the uptake of DiI-oxLDL. The results showed no significant difference of the fluorescent intensity between WT and ALDH2$^{-/-}$ mice (Fig. 5A–B). Furthermore, BMDMs were treated with oxLDL (80 μg/ml) for 24 h to induce foam cell formation as previously reported [28]. ORO staining revealed little difference of foam cell formation between WT and ALDH2$^{-/-}$ mice (Fig. 5C–D). These results indicated that the effect of ALDH2 deficiency on plaque instability might not be attributed to foam cell formation in macrophages.

3.6. Effect of ALDH2 deficiency on VSMC senescence

Given that VSMC senescence plays an important role in promoting atherosclerotic vulnerability [7,29], we next detected the effect of ALDH2 overexpression on VSMC senescence following treatment with oxLDL (80 μg/ml) for 72 h as previously reported [29]. First, ALDH2 siRNA was transfected to knockdown ALDH2 in VSMCs (Fig. 6A). After 72 h of oxLDL treatment, VSMC showed significantly increased SA-β-gal positive cells, while ALDH2 knockdown significantly aggravated the effect of oxLDL (Fig. 6B–C). Then ALDH2 lentivirus was infected to obtain ALDH2 overexpressed VSMCs (Fig. 6D). After 72 h of oxLDL treatment, ALDH2 overexpression significantly reversed the inductive effect of oxLDL on VSMC senescence (Fig. 6E–F). As p53/p21 and p16 were considered as alternative markers for cellular senescence in human atheroma [30,31], we next detected the expression of senescence related markers p53/p21/p16. The Western blotting results showed clearly that ALDH2 overexpression inhibited p53/p21/p16 expression compared with Control group (Fig. 6G–H). These results demonstrated the inhibitory effect of ALDH2 on VSMC senescence.

3.7. The regulative effect of ALDH2 on VSMC senescence is dependent on mitochondrial ROS

Since a crosstalk between mitochondrial ROS (mROS) and p53/p21/p16 exists in the process of VSMC senescence [32,33], we then detected mROS generation by both DHE and mitoSOX staining. The results showed that ALDH2 knockdown significantly aggravated oxLDL-induced mROS overproduction, showed as increased DHE and mitoSOX fluorescent intensity (Fig. 7A–D). Besides, ALDH2 overexpression significantly reversed oxLDL-induced mROS overproduction, showed as decreased DHE and mitoSOX fluorescent intensity (Fig. 7E–H). To further elucidate whether mROS is dispensable in mediating the regulative effect of ALDH2 on VSMC senescence, the mROS scavenger mitoTEMPO (10 μM) was used as previously reported [34] and further results showed that mitoTEMPO administration significantly inhibited the generation of mROS after oxLDL treatment in both NC and ALDH2 knockdown group to a similar level (Fig. 8A–D). Moreover, mitoTEMPO administration almost completely reversed the aggravated effect of ALDH2 knockdown on VSMC senescence (Fig. 8E–F). Collectively, these data revealed that ALDH2 protects against oxLDL-induced VSMC senescence by eliminating mROS overproduction.

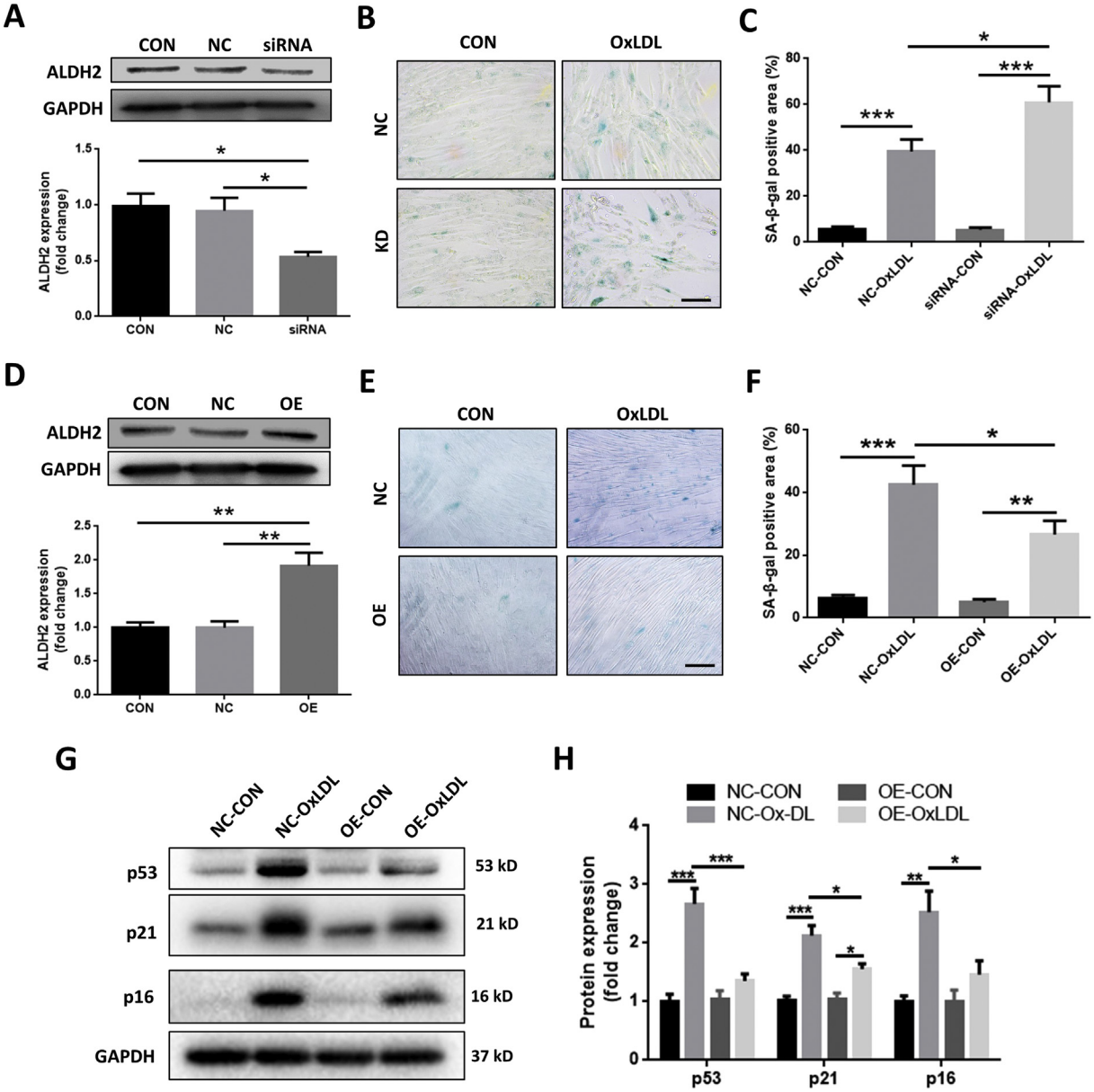

Fig. 6. The effect of ALDH2 knockdown and overexpression on VSMC senescence after oxLDL treatment. A: Representative Western blotting pictures and statistical analyses of ALDH2 expression after ALDH2 siRNA transfection; B: Representative pictures of SA-β-gal staining in VSMCs after 80 μg/ml oxLDL treatment for 72 h, scale bar = 100 μm; C: Statistical analyses of SA-β-gal staining; D: Representative Western blotting pictures and statistical analyses of ALDH2 expression after ALDH2 lentivirus infection; E: Representative pictures of SA-β-gal staining in VSMCs after 80 μg/ml oxLDL treatment for 72 h, scale bar = 100 μm; D: Statistical analyses of SA-β-gal staining; G: Representative Western blotting pictures of p53, p21, and p16 in NC and OE group with or without 80 μg/ml oxLDL treatment for 72 h; H: Statistical analyses of the expression of p53, p21, and p16. Mean ± SEM, n = 5–6 for all groups. $^{*}p < 0.05$, $^{**}p < 0.01$, $^{***}p < 0.001$.

4. Discussion

Several previous studies have revealed a protective role of ALDH2 in the suppression of atherosclerotic lesion progression or plaque vulnerability, although the mechanisms remain somewhat elusive. More importantly, the relationship between genetic ALDH2 mutation and atherosclerosis remain largely unknown. Findings of our study revealed that ALDH2 deficiency in the atherosclerosis-prone ApoE$^{-/-}$ mice decreased the atherosclerotic plaque area while it paradoxically promoted the atherosclerotic plaque instability. Further results revealed that ALDH2 expression decreased in aorta of old-aged ApoE$^{-/-}$ mice with advanced atherosclerotic lesions compared with young mice. However, the change of ALDH2 expression varied in the in vitro study, with an increase in macrophages and a decrease in VSMCs treated with oxLDL, suggesting a disparate role for ALDH2 in different cell types in the pathogenesis of atherosclerosis. Our data further revealed little difference in foam cell formation of BMDMs treated with oxLDL. Interestingly, VSMC senescence seems to be involved in this process. ALDH2 overexpression using lentivirus overtly inhibited oxLDL-induced VSMC senescence, possibly via a ROS-mediated p53/p21/p16 mechanism. Taken together, these results elucidated that ALDH2 deficiency decreased atherosclerotic plaque area while promoting plaque instability possibly via accelerating mROS-mediated VSMC senescence. To the best of our knowledge, this is the first study revealing the effect of genetic ALDH2 deficiency on foam cell formation in macrophages and VSMC senescence in the pathogenesis of atherosclerosis.

As an important metabolic enzyme and endogenous protective factor, ALDH2 may protect against various forms of CVDs [11,16,20]. Importantly, several studies have demonstrated that ALDH2 mutation was positively associated with the prevalence of CHD [35,36] and

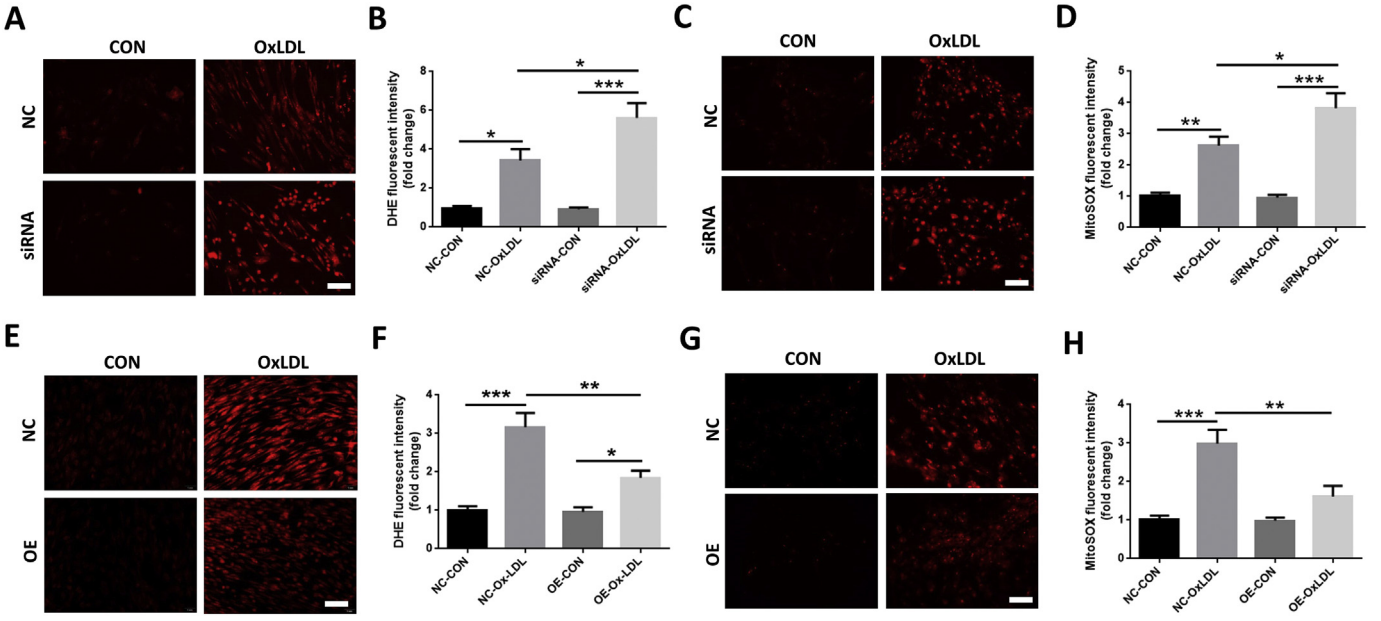

Fig. 7. The effect of ALDH2 overexpression on mROS generation after oxLDL treatment. A, E: Representative pictures of DHE staining after 80 μg/ml oxLDL treatment for 72 h, scale bar = 100 μm; B, F: Statistical analyses of DHE fluorescent density (fold change). C, G: Representative pictures of mitoSOX staining after 80 μg/ml oxLDL treatment for 72 h, scale bar = 100 μm; D, H: Statistical analyses of mitoSOX fluorescent density (fold change). Mean ± SEM, $n = 6$ for all groups. $^{*}p < 0.05$, $^{**}p < 0.01$, $^{***}p < 0.001$.

stroke [18,19]. As the major cause of CHD, atherosclerosis was expected to be associated with ALDH2 mutation. However, it remains controversial to some extent whether ALDH2 mutation was associated with atherosclerosis from the clinical perspective. A clinical retrospective study revealed that ALDH2 Glu504Lys mutation was associated with a higher carotid intima-media thickness in Chinese Han population with essential hypertension [37]. However, another study revealed the opposite result that ALDH2 mutation seemed to be associated with less severity of carotid atherosclerosis in patients with ALDH2 mutations compared with the wild type population [38]. Another independent study revealed no association of ALDH2 mutation and the coronary atherosclerosis severity [39]. Therefore, the relationship between ALDH2 polymorphism and clinical atherosclerosis warrants further study. Moreover, the role of ALDH2 in the pathogenesis of experimental atherosclerosis remains largely unknown. It was reported that ALDH2 activation by Alda-1 inhibited atherosclerosis area with little influence on lipid profile or plaque stability in $ApoE^{-/-}$ mice [22], while another study revealed that ALDH2 knockdown by lentivirus led to an increased plaque area and more unstable plaque, the effects of which were associated with aggravated inflammation in endothelial cells [23]. Unexpectedly, our study using $ALDH2^{-/-}ApoE^{-/-}$ mice revealed an opposite result that ALDH2 deficiency decreased atherosclerotic plaque area compared with $ApoE^{-/-}$ mice, which was in line with our earlier study that ALDH2 deficiency in an atherosclerosis-prone low density lipoprotein receptor (LDLR) knockout background decreased atherosclerotic plaque area compared with $ALDH2^{+/+}LDLR^{-/-}$ mice (unpublished data).

Previous pathological examinations in human have demonstrated that components of plaques rather than size of plaques play a more prominent role in the development of ACS, as increased plaque vulnerability serves as a major cause for atherosclerotic plaque disruption [3,40]. Plaque vulnerable to disruption is characterized as increased content of lipids and macrophages and reduced content of collagen and SMCs [40]. Consistent with Pan's study [23], our study revealed that atherosclerotic lesions in $ALDH2^{-/-}ApoE^{-/-}$ mice displayed a more vulnerable status than that of $ApoE^{-/-}$ mice, manifested as bigger necrotic core size, thinner fibrous cap, lesser collagen content, more macrophage filtration and decreased SMCs in the lesions. Lipid profile revealed that ALDH2 might regulate lipid metabolism, evidenced by increased serum TG levels, decreased TC and HDL-C levels in $ALDH2^{-/-}ApoE^{-/-}$ mice compared with $ApoE^{-/-}$ mice. The effect of ALDH2 deficiency on decreasing HDL-C level was in line with several previous studies [36,41], accounting for the increased necrotic core size and plaque vulnerability in $ALDH2^{-/-}ApoE^{-/-}$ mice.

Atherosclerotic lesion formation is associated with accumulation of oxidized lipids, the products of which, particularly aldehydes, stimulate cytokine production and enhance monocyte adhesion [25,42]. Endothelial cells, macrophages and VSMCs are the most important and well-studied cell types involved in the pathogenesis of atherosclerosis. The protective role of ALDH2 in inhibiting inflammatory response in endothelial cells were noted [23] although the effect on foam cell formation in macrophages remains unclear. In our study, ALDH2 expression was overtly elevated after 80 μg/ml oxLDL treatment, suggesting a compensatory role for ALDH2 in the protection against oxLDL challenge. Though ALDH2 deficiency abruptly promoted macrophage content in the lesion compared with control mice, little difference was found as to foam cell formation in macrophages. As for VSMCs, it was reported that ALDH2 activation by Alda-1 inhibited oxLDL-induced VSMC apoptosis and ER stress and subsequent plaque vulnerability [12]. Apart from VSMC apoptosis, VSMC senescence also plays an important role in promoting plaque instability [7,29]. Given that ALDH2 might play an important role in the process of aging [43], we therefore investigated the role of ALDH2 in VSMC senescence. Firstly, our results revealed that ALDH2 expression was decreased in an in vitro oxLDL-treated VSMC senescence model, in line with the previous study in human atheroma-derived VSMCs [44]. Our data went on to reveal that ALDH2 overexpression protected against oxLDL-induced VSMC senescence, manifested as decreased SA-β-gal positive cells and levels of senescence markers p53/p21/p16. As the main substrate for ALDH2 enzyme, ROS are known to regulate VSMC senescence via cross-talk between p53/p21 and p16 [32,33]. Our data clearly suggested that ALDH2 inhibited mROS generation triggered by oxLDL treatment. Our further results proved clearly that ALDH2 overexpression inhibited mROS generation induced by oxLDL treatment compared with control group, and mROS scavenger mitoTEMPO almost completely reversed the aggravated effect of ALDH2 knockdown on VSMC senescence.

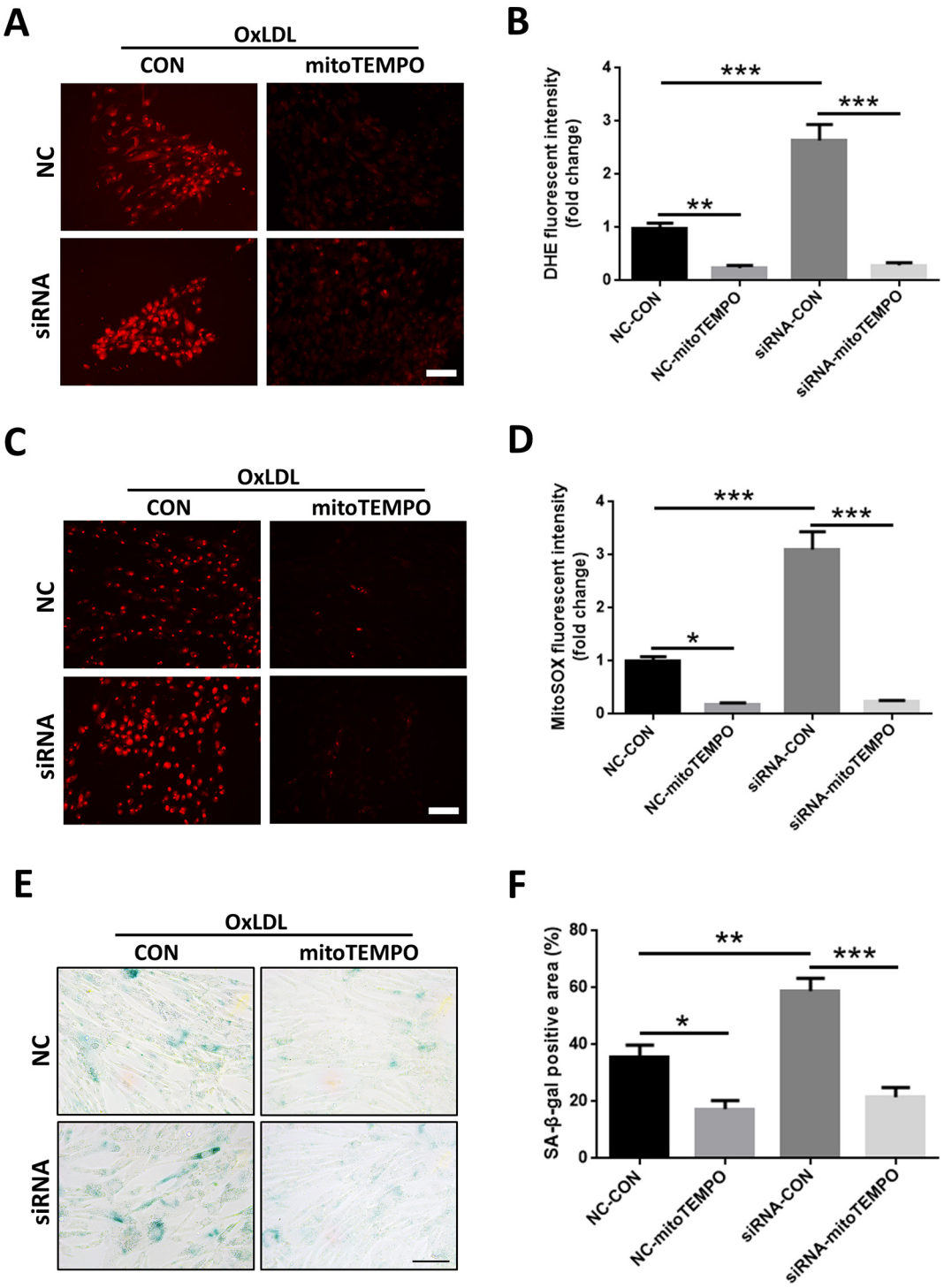

Fig. 8. The effect of mROS scavenger mitoTEMPO on VSMC senescence after oxLDL treatment. A: Representative pictures of DHE staining after 80 μg/ml oxLDL treatment for 72 h in NC and ALDH2 siRNA groups with or without mitoTEMPO, scale bar = 100 μm; B: Statistical analyses of DHE fluorescent density (fold change); C: Representative pictures of mitoSOX staining after 80 μg/ml oxLDL treatment for 72 h in NC and ALDH2 siRNA groups with or without mitoTEMPO, scale bar = 100 μm; D: Statistical analyses of mitoSOX fluorescent density (fold change). E: Representative pictures of SA-β-gal staining in VSMCs after 80 μg/ml oxLDL treatment for 72 h in NC and ALDH2 siRNA groups with or without mitoTEMPO, scale bar = 100 μm; F: Statistical analyses of SA-β-gal staining. Mean ± SEM, $n = 5–6$ for all groups. $^{*}p < 0.05$, $^{**}p < 0.01$, $^{***}p < 0.001$.

In conclusion, data from our current study revealed that ALDH2 deficiency decreased atherosclerotic plaque area while promoting plaque instability, possibly through a mechanism related to VSMC senescence in a mROS-mediated p53/p21/p16 manner. Although much in-depth study is warranted to explore the correlation between ALDH2 mutation and atherosclerotic plaque formation, findings from our present study should shed some lights towards a better understanding of the beneficial effect of ALDH2 in the pathogenesis of atherosclerosis.

Transparency document

The Transparency document associated with this article can be

found, in online version.

Author contributions

HZ, YZ, JG, XZ and YZ were involved in the conception and design of the study; HZ, ZW, ZD, CW, QC, FF, XP were involved in performance of experiments and data analysis; JZ, XL, MY, and XS acquired the data; HZ and YZ wrote the manuscript.

Funding sources

This work was supported by grants from the National Key R&D Program of China (2016YFC 1301200), National Natural Science Foundation of China (81570224, 81770261, and 91639104) and the Foundation for Innovative Research Groups of the National Natural Science Foundation of China (81521001).

Competing interests

The authors have declared that no competing interests exist.

References

[1] P. Libby, Y. Okamoto, V.Z. Rocha, E. Folco, Inflammation in atherosclerosis: transition from theory to practice, CIRC J. 74 (2010) 213–220.
[2] A.C. Newby, S.J. George, Y. Ismail, J.L. Johnson, G.B. Sala-Newby, A.C. Thomas, Vulnerable atherosclerotic plaque metalloproteinases and foam cell phenotypes, Thromb. Haemost. 101 (2009) 1006–1011.
[3] I. Rohwedder, E. Montanez, K. Beckmann, E. Bengtsson, P. Duner, J. Nilsson, O. Soehnlein, R. Fassler, Plasma fibronectin deficiency impedes atherosclerosis progression and fibrous cap formation, EMBO Mol. Med. 4 (2012) 564–576.
[4] I. Zeller, S. Srivastava, Macrophage functions in atherosclerosis, Circ. Res. 115 (2014) e83–e85.
[5] A.C. Newby, A.B. Zaltsman, Fibrous cap formation or destruction–the critical importance of vascular smooth muscle cell proliferation, migration and matrix formation, Cardiovasc. Res. 41 (1999) 345–360.
[6] M. Grootaert, M. Moulis, L. Roth, W. Martinet, C. Vindis, M.R. Bennett, G. De Meyer, Vascular smooth muscle cell death, autophagy and senescence in atherosclerosis, Cardiovasc. Res. 114 (2018) 622–634.
[7] J. Wang, A.K. Uryga, J. Reinhold, N. Figg, L. Baker, A. Finigan, K. Gray, S. Kumar, M. Clarke, M. Bennett, Vascular smooth muscle cell senescence promotes atherosclerosis and features of plaque vulnerability, Circulation 132 (2015) 1909–1919.
[8] Y. Xiong, Y. Yu, J.P. Montani, Z. Yang, X.F. Ming, Arginase-II induces vascular smooth muscle cell senescence and apoptosis through p66Shc and p53 independently of its l-arginine ureahydrolase activity: implications for atherosclerotic plaque vulnerability, J. Am. Heart Assoc. 2 (2013) e000096.
[9] P.M. Nilsson, Early vascular aging (EVA): consequences and prevention, Vasc. Health Risk Manag. 4 (2008) 547–552.
[10] M. Aikawa, P. Libby, The vulnerable atherosclerotic plaque: pathogenesis and therapeutic approach, Cardiovasc. Pathol. 13 (2004) 125–138.
[11] C.H. Chen, L. Sun, D. Mochly-Rosen, Mitochondrial aldehyde dehydrogenase and cardiac diseases, Cardiovasc. Res. 88 (2010) 51–57.
[12] M.Y. Yang, Y.B. Wang, B. Han, B. Yang, Y.W. Qiang, Y. Zhang, Z. Wang, X. Huang, J. Liu, Y.D. Chen, J. Ren, F. Cao, Y. Xu, Activation of aldehyde dehydrogenase 2 slows down the progression of atherosclerosis via attenuation of ER stress and apoptosis in smooth muscle cells, Acta Pharmacol. Sin. 39 (2018) 48–58.
[13] Y.Y. Li, H. Wang, J.J. Wu, H.J. Kim, X.X. Yang, H.Y. Geng, G. Gong, ALDH2 gene G487A polymorphism and coronary artery disease: a meta-analysis including 5644 participants, J. Cell. Mol. Med. 22 (2018) 1666–1674.
[14] X. Liu, X. Sun, H. Liao, Z. Dong, J. Zhao, H. Zhu, P. Wang, L. Shen, L. Xu, X. Ma, C. Shen, F. Fan, C. Wang, K. Hu, Y. Zou, J. Ge, J. Ren, A. Sun, Mitochondrial aldehyde dehydrogenase 2 regulates revascularization in chronic ischemia: potential impact on the development of coronary collateral circulation, Arterioscler. Thromb. Vasc. Biol. 35 (2015) 2196–2206.
[15] H. Ma, R. Guo, L. Yu, Y. Zhang, J. Ren, Aldehyde dehydrogenase 2 (ALDH2) rescues myocardial ischaemia/reperfusion injury: role of autophagy paradox and toxic aldehyde, Eur. Heart J. 32 (2011) 1025–1038.
[16] Y. Zhang, J. Ren, ALDH2 in alcoholic heart diseases: molecular mechanism and clinical implications, Pharmacol. Ther. 132 (2011) 86–95.
[17] C. Wang, F. Fan, Q. Cao, C. Shen, H. Zhu, P. Wang, X. Zhao, X. Sun, Z. Dong, X. Ma, X. Liu, S. Han, C. Wu, Y. Zou, K. Hu, J. Ge, A. Sun, Mitochondrial aldehyde dehydrogenase 2 deficiency aggravates energy metabolism disturbance and diastolic dysfunction in diabetic mice, J. Mol. Med. (Berl.) 94 (2016) 1229–1240.
[18] Y.F. Sung, C.C. Lu, J.T. Lee, Y.J. Hung, C.J. Hu, J.S. Jeng, H.Y. Chiou, G.S. Peng, Homozygous ALDH2*2 is an independent risk factor for ischemic stroke in Taiwanese men, Stroke 47 (2016) 2174–2179.
[19] Y. Li, S.L. Liu, S.H. Qi, ALDH2 protects against ischemic stroke in rats by facilitating 4-HNE clearance and AQP4 down-regulation, Neurochem. Res. (2018) (Epub ahead of print).
[20] J. Pang, J. Wang, Y. Zhang, F. Xu, Y. Chen, Targeting acetaldehyde dehydrogenase 2 (ALDH2) in heart failure-recent insights and perspectives, Biochim. Biophys. Acta 1863 (2017) 1933–1941.
[21] X. Liu, A. Sun, Aldehyde dehydrogenase-2 roles in ischemic cardiovascular disease, Curr. Drug Targets 18 (2017) 1817–1823.
[22] A. Stachowicz, R. Olszanecki, M. Suski, A. Wisniewska, J. Toton-Zuranska, J. Madej, J. Jawien, M. Bialas, K. Okon, M. Gajda, K. Glombik, A. Basta-Kaim, R. Korbut, Mitochondrial aldehyde dehydrogenase activation by Alda-1 inhibits atherosclerosis and attenuates hepatic steatosis in apolipoprotein E-knockout mice, J. Am. Heart Assoc. 3 (2014) e001329.
[23] C. Pan, J.H. Xing, C. Zhang, Y.M. Zhang, L.T. Zhang, S.J. Wei, M.X. Zhang, X.P. Wang, Q.H. Yuan, L. Xue, J.L. Wang, Z.Q. Cui, Y. Zhang, F. Xu, Y.G. Chen, Aldehyde dehydrogenase 2 inhibits inflammatory response and regulates atherosclerotic plaque, Oncotarget 7 (2016) 35562–35576.
[24] A. Yoshida, I.Y. Huang, M. Ikawa, Molecular abnormality of an inactive aldehyde dehydrogenase variant commonly found in Orientals, Proc. Natl. Acad. Sci. U. S. A. 81 (1984) 258–261.
[25] S. Srivastava, E. Vladykovskaya, O.A. Barski, M. Spite, K. Kaiserova, J.M. Petrash, S.S. Chung, G. Hunt, B. Dawn, A. Bhatnagar, Aldose reductase protects against early atherosclerotic lesion formation in apolipoprotein E-null mice, Circ. Res. 105 (2009) 793–802.
[26] J. Weischenfeldt, B. Porse, Bone marrow-derived macrophages (BMM): isolation and applications, CSH Protoc. 2008 (2008) (pdb.prot5080).
[27] K.J. Moore, I. Tabas, Macrophages in the pathogenesis of atherosclerosis, Cell 145 (2011) 341–355.
[28] A. Laguna-Fernandez, A. Checa, M. Carracedo, G. Artiach, M.H. Petri, R. Baumgartner, M.J. Forteza, X. Jiang, T. Andonova, M.E. Walker, J. Dalli, H. Arnardottir, A. Gistera, S. Thul, C.E. Wheelock, G. Paulsson-Berne, D. Ketelhuth, G.K. Hansson, M. Back, ERV1/ChemR23 signaling protects from atherosclerosis by modifying oxLDL uptake and phagocytosis in macrophages, Circulation (2018) (Epub ahead of print).
[29] Z. Luo, W. Xu, S. Ma, H. Qiao, L. Gao, R. Zhang, B. Yang, Y. Qiu, J. Chen, M. Zhang, B. Tao, F. Cao, Y. Wang, Moderate autophagy inhibits vascular smooth muscle cell senescence to stabilize progressed atherosclerotic plaque via the mTORC1/ULK1/ATG13 signal pathway, Oxidative Med. Cell. Longev. 2017 (2017) 3018190.
[30] T. Kunieda, T. Minamino, J. Nishi, K. Tateno, T. Oyama, T. Katsuno, H. Miyauchi, M. Orimo, S. Okada, M. Takamura, T. Nagai, S. Kaneko, I. Komuro, Angiotensin II induces premature senescence of vascular smooth muscle cells and accelerates the development of atherosclerosis via a p21-dependent pathway, Circulation 114 (2006) 953–960.
[31] M. Vogt, C. Haggblom, J. Yeargin, T. Christiansen-Weber, M. Haas, Independent induction of senescence by p16INK4a and p21CIP1 in spontaneously immortalized human fibroblasts, Cell Growth Differ. 9 (1998) 139–146.
[32] B. Liu, Y. Chen, C.D. St, ROS and p53: a versatile partnership, Free Radic. Biol. Med. 44 (2008) 1529–1535.
[33] D.J. Li, F. Huang, M. Ni, H. Fu, L.S. Zhang, F.M. Shen, alpha7 nicotinic acetylcholine receptor relieves angiotensin II-induced senescence in vascular smooth muscle cells by raising nicotinamide adenine dinucleotide-dependent SIRT1 activity, Arterioscler. Thromb. Vasc. Biol. 36 (2016) 1566–1576.
[34] A.E. Vendrov, K.C. Vendrov, A. Smith, J. Yuan, A. Sumida, J. Robidoux, M.S. Runge, N.R. Madamanchi, NOX4 NADPH oxidase-dependent mitochondrial oxidative stress in aging-associated cardiovascular disease, Antioxid. Redox Signal. 23 (2015) 1389–1409.
[35] Y.J. Guo, L. Chen, Y.P. Bai, L. Li, J. Sun, G.G. Zhang, T.L. Yang, J. Xia, Y.J. Li, X.P. Chen, The ALDH2 Glu504Lys polymorphism is associated with coronary artery disease in Han Chinese: relation with endothelial ADMA levels, Atherosclerosis 211 (2010) 545–550.
[36] L. Xu, G. Zhao, J. Wang, C. Shen, X. Li, F. Lu, H. Jiang, G. Liu, K. Hu, Y. Tang, A. Sun, J. Ge, Impact of genetic variation in aldehyde dehydrogenase 2 and alcohol consumption on coronary artery lesions in Chinese patients with stable coronary artery disease, Int. Heart J. 59 (2018) 689–694.
[37] X.X. Ma, S.Z. Zheng, Y. Shu, Y. Wang, X.P. Chen, Association between carotid intima-media thickness and aldehyde dehydrogenase 2 Glu504Lys polymorphism in Chinese Han with essential hypertension, Chin. Med. J. 129 (2016) 1413–1418.
[38] M. Narita, K. Kitagawa, Y. Nagai, H. Hougaku, H. Hashimoto, M. Sakaguchi, X. Yang, T. Takeshita, K. Morimoto, M. Matsumoto, M. Hori, Effects of aldehyde dehydrogenase genotypes on carotid atherosclerosis, Ultrasound Med. Biol. 29 (2003) 1415–1419.
[39] F. Xu, Y.G. Chen, Y.J. Geng, H. Zhang, C.X. Jiang, Y. Sun, R.J. Li, M.B. Sagar, L. Xue, Y. Zhang, The polymorphism in acetaldehyde dehydrogenase 2 gene, causing a substitution of Glu & Lys(504), is not associated with coronary atherosclerosis severity in Han Chinese, Tohoku J. Exp. Med. 213 (2007) 215–220.
[40] G.K. Hansson, P. Libby, I. Tabas, Inflammation and plaque vulnerability, J. Intern. Med. 278 (2015) 483–493.
[41] M. Wada, M. Daimon, M. Emi, H. Iijima, H. Sato, S. Koyano, K. Tajima, T. Kawanami, K. Kurita, S.C. Hunt, P.N. Hopkins, I. Kubota, S. Kawata, T. Kato, Genetic association between aldehyde dehydrogenase 2 (ALDH2) variation and high-density lipoprotein cholesterol (HDL-C) among non-drinkers in two large population samples in Japan, J. Atheroscler. Thromb. 15 (2008) 179–184.
[42] K. Uchida, Role of reactive aldehyde in cardiovascular diseases, Free Radic. Biol. Med. 28 (2000) 1685–1696.
[43] Y. Zhang, S.L. Mi, N. Hu, T.A. Doser, A. Sun, J. Ge, J. Ren, Mitochondrial aldehyde dehydrogenase 2 accentuates aging-induced cardiac remodeling and contractile dysfunction: role of AMPK, Sirt1, and mitochondrial function, Free Radic. Biol. Med. 71 (2014) 208–220.
[44] L.E. Viiri, L.E. Full, T.J. Navin, S. Begum, A. Didangelos, N. Astola, R.K. Berge, I. Seppala, J. Shalhoub, I.J. Franklin, M. Perretti, T. Lehtimaki, A.H. Davies, R. Wait, C. Monaco, Smooth muscle cells in human atherosclerosis: proteomic profiling reveals differences in expression of Annexin A1 and mitochondrial proteins in carotid disease, J. Mol. Cell. Cardiol. 54 (2013) 65–72.